

Electronic Supplementary Material (ESI) for ChemComm.

This journal is © The Royal Society of Chemistry 2022

Electronic Supplementary Information

An Ultrasensitive Electrochemical Biosensor for MicroRNA-21 Detection Via AuNPs/GAs and Y-shaped DNA Dual-Signal Amplification Strategy

Congjuan He ‡^a, Jiaying Zhao ‡^a, Yanyi Long ^a, Huisi Yang ^a, Jiangbo Dong ^a, Huan Liu ^d, Zhikun Hu ^a, Mei Yang ^a, Danqun Huo ^{*a, c}, Changjun Hou ^{*a, b}

a. Key Laboratory for Biorheological Science and Technology of Ministry of Education, State and Local Joint Engineering Laboratory for Vascular Implants, Bioengineering College of Chongqing University, Chongqing 400044, PR China.

b. Chongqing Key Laboratory of Bio-perception & Intelligent Information Processing, School of Microelectronics and Communication Engineering, Chongqing University, Chongqing, 400044, PR China.

c. National Facility for Translational Medicine, Shanghai Jiao Tong University, Shanghai, 200240, PR China

d. Chongqing Institute for Food and Drug Control, Chongqing 401121, PR China

* Corresponding author. E-mail addresses: houcj@cqu.edu.cn (C.J. Hou), huodq@cqu.edu.cn (D.Q. Huo). Tel: +86 23 6510 2507

† Electronic supplementary information (ESI) available: Details of experimental procedures and additional figures. See DOI: 10.1039/d0cc04855k. See DOI: 10.1039/x0xx00000x

‡ Congjuan He and Jiaying Zhao contributed equally to this work.

1. Reagents

Graphene oxide (GO) was purchased from Nanjing Xianfeng Nanotech Co., Ltd (Nanjing, China). Chlorauric acid trihydrate ($\text{HAuCl}_4 \cdot 3\text{H}_2\text{O}$) was bought from Aladdin Biochemical Technology Co., Ltd (Shanghai, China). Phosphate buffer saline (PBS, 0.01M, PH =7.4) was bought in Beijing Ding Guo Chang sheng Biotechnology Co., Ltd (Beijing, China). All the oligonucleotide sequences purified by HPLC were synthesized and purified in Sangon Biotech Co., Ltd (Shanghai, China) and were listed in **Table S1**. Normal human serum was purchased in Beijing Solaibao Technology Co., Ltd (Beijing, China). All the other reagents were analytically pure and can be used directly. All aqueous liquid was prepared with deionized water (DI, 18.2 M Ω ·cm) purified with a Millipore.

Table S1. Sequences of the oligonucleotides used in the experiment ¹

Name	Sequence (5'-3')
miR-21	UAGCUU AUCAG ACUGAU GUUGA
H1	TCAACATCAGTCTGATAAGCTAGTAACCCGGTTAGCTTAT CAGACTGA
H2	CTGATAAGCTAACCGGGTTACTGATGTTGAGTAACCC GGTTAGCTT
H3	ACCGGGTACTCAACATCAGTTAGCTTATCAGACTGATGTTGAGTAAC CCATGTCCATGTGTAGA
Probe DNA	HS-TCTACACATGGACATGG
miR-21-SM	UAGCUUAUCAGACUGAUGUUCA
miR-21-TM	UAGCUUAUCAGACUCAUCUUCA
miR-155	UUA AUGCUAAUCGUGAUAGGGGU
miR-16	UAGCAGCACGUAAAUAUUGGCG
Let-7a	UGAGGUAGUAGGUUGUAUAGUU

SM (single-base mismatched), TM (three-base mismatched)

2. Apparatus

The morphology and elemental composition of the prepared materials were analyzed by field-emission scanning electron microscope (FESEM, Nova 400), energy dispersive spectroscopy (EDS), Raman spectrometer and X-Ray Diffractometer (XRD). All the electrochemical tests were performed on a CHI 760E electrochemical workstation (Shanghai Chenhua apparatus Co., Ltd, China) consisting of a traditional three-electrode system which includes a modified glassy carbon electrode (GCE, $\Phi=3\text{mm}$) as the working electrode, a silver/silver chloride (Ag/AgCl) reference electrode and a platinum wire (counter electrode). Besides, $[\text{Fe}(\text{CN})_6]^{3-/4-}$ solution (5 mM) containing 0.1 M KCl (1:1 v/v) was used as a test solution for cyclic voltammetry (CV) and electrochemical impedance spectroscopy (EIS). The potential of CVs ranges from -0.2 to +0.6 V at the scanning rate of 0.5 V/s, and EIS was conducted in the frequency domain of 1~100000 Hz with an amplitude of 0.005V. Afterwards, differential pulse voltammetry (DPV) was operated in 0.01 M phosphate buffer saline (PBS, pH=7.4) with a scanning range of -0.8V ~ 0.2V and pulse amplitude of 0.025V.

3. Experimental section

3.1 Synthesis of GAs

GAs was fabricated through a one-pot solvothermal reaction with a slight modification ². Briefly, 45 mg graphene oxide (GO) was added into 30 mL distilled water under ultrasonic for 1 h to form a uniform GO dispersion. Then, the GO dispersion was transferred into a 50 mL Teflon-lined stainless-steel reaction kettle and heated at a temperature of 180 °C for 12 h in an oven. After being cooled to room temperature, the black products were collected by centrifugation at 11000 rpm for 15 min and cleaned with DI water 3 ~ 4 times. After freeze-drying for 12 h, the porous GAs was obtained.

3.2 Preparation of the Y-shaped DNA nanostructure

Before the experiment, each kind of well-designed hairpin probe (H1, H2, and H3) was annealed at 95 °C for 10 min and then slowly cooled to 25 °C to hold a stable secondary structure. Then, the hairpin probes H1 (100 nM), H2 (100 nM) and H3 (100 nM) were mixed well with different concentrations of miR-21 in TM buffer (10 mM Tris - HCl, 50 mmol/L MgCl₂, 30 mM TCEP; pH = 8), placing at 25°C for 1.5 h to form the Y-shaped DNA nanostructure with three branches during the CHA process.

3.3 Proof of the formation of Y-shaped DNA nanostructure

The feasibility of the proposed CHA amplification strategy was confirmed through a 10% polyacrylamide gel electrophoretic analysis (PAGE). Briefly, 10 μ L incubation products and 2 μ L loading buffer were fully mixed and loaded onto the relevant lane. Then, the electrophoresis was run in 1x TBE buffer at 110 V for 70 min. After dyeing by Gel Red for 15min, the gel imaging was performed under a gel imager (GBOX-F3-E).

In order to further verify the feasibility of this strategy, we coated the sample solution on the mica sheet and observed the morphology of Y-shaped DNA nanostructure generated in the CHA reaction system by atomic force microscope (AFM, Bruker Icon).

3.4 Preparation of the modified electrode

Before surface modification of the bare glassy carbon electrode (GCE, $\phi = 3\text{mm}$), the electrode was polished carefully with alumina powder successively and then treated with ultrasound in ethanol and DI water for 10 s respectively to remove the redundant powder. After drying under nitrogen flow, the GCE was modified with 10 μ L of the GAs suspension (1mg/mL) by drop-casting and dried at 37 °C. Then, the obtained GAs/GCE was immersed in a mixture of 0.01 M Na₂SO₄, 0.01 M H₂SO₄ and 2 mM HAuCl₄, and electrodeposited for 200 s at -0.2 V by chronoamperometry (i-t technique). The modified electrode was named as AuNPs/GAs/GCE finally.

3.5 Fabrication process of the proposed electrochemical biosensor

Firstly, 5 μ L 1 μ M thiol-modified capture probe DNA was dropped on the surface

of AuNPs/GAs/GCE and kept at 25 °C for 90 min. Through rinsing, the redundant probes were eliminated. Then, using 1 mM MCH to block the other active sites. Subsequently, 5 μ L of the Y-shaped DNA probe in the homogeneous solution hybridized with the capture probe DNA for 90 min at room temperature (25 °C). Following by a treatment of 5 μ L PBS containing 1mM MB for 40 min in dark at room temperature. Finally, the excess MB on the electrode was washed with DI water and measured at 0.01 M PBS (pH=7.4) with DPV.

3.6 Recovery of miRNA-21 from normal human serum by adding standard

The standard addition method was used to detect miRNA-21 in normal human serum. To be specific, the serum was diluted 30 times with PBS for further use. After that, three concentrations of miR-21 (50 nM, 5 nM and 0.5nM) were severally added into the mixed system of H1, H2 and H3. After incubation, DPV was measured in the diluted serum. The recovery was calculated according to the relationship between the current value and miR-21 concentration in the standard linear calibration curve.

4. Results and discussion

4.1 CV studies of sensing electrodes.

CV studies of GAs/GCE and AuNPs/GAs/GCE at different sweep speeds in ferrocyanide were performed to illustrate the important role of AuNPs/GAs in the sensing strategy. An increase in the redox peak current was observed as the scan rate increased (from 10 to 250 mV/s for GAs/GCE and from 10 to 325 mV/s for AuNPs/GAs/GCE) in **Fig. S1A** and **Fig. S1C**. As displayed in **Fig. S1B** and **Fig. S1D**, there was a good linear relationship between peak current (I_p) and the square root of the scan rate ($v^{1/2}$) and the corresponding linear equations were as follows: $I_{pa} = 18.22v^{1/2} + 0.1845$ ($R^2 = 0.9937$), $I_{pc} = -17.28v^{1/2} - 0.9059$ ($R^2 = 0.9914$) for GAs/GCE and $I_{pa} = 22.24v^{1/2} - 10.97$ ($R^2 = 0.9995$), $I_{pc} = -20.84v^{1/2} + 5.425$ ($R^2 = 0.9999$) for AuNPs/GAs/GCE, indicating that the oxidation-reduction reaction was a diffusion-controlled process at the interface between GAs and AuNPs/GAs modified electrodes.

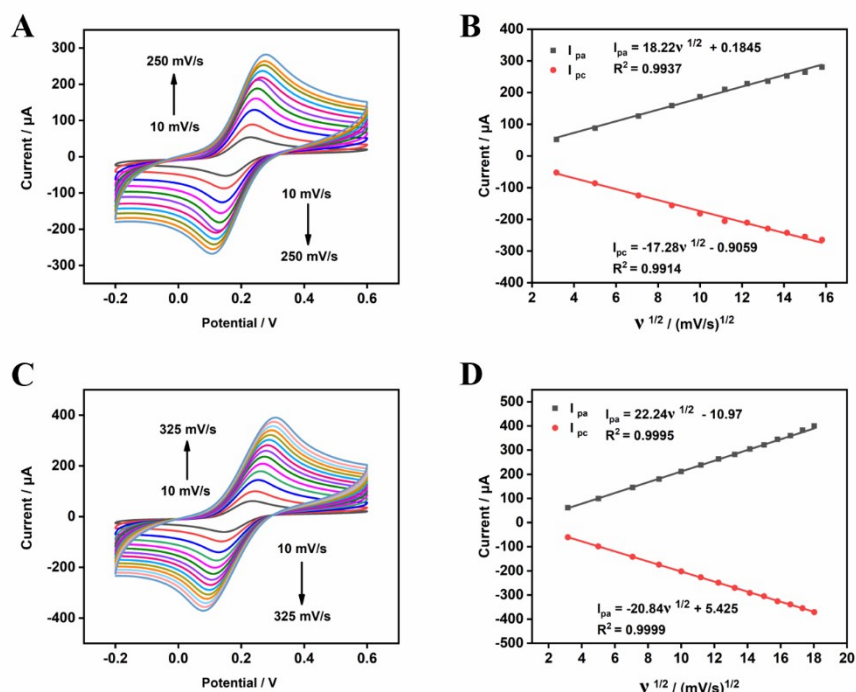


Fig. S1 CV curves of GAs/GCE (A) and AuNPs/GAs/GCE (C) at different scan rates in 5 mM $[\text{Fe}(\text{CN})_6]^{3-/4-}$ containing 0.1 M KCl; Corresponding linear correlation plots between the square root of the scan rate ($v^{1/2}$) and the oxidation peak current for GAs/GCE (B) and AuNPs/GAs/GCE (D).

Thus, the anode peak currents (**Fig. S2**) were used to calculate the effective area (A) of the modified electrode according to the Randles-Sevcik equation: $I_p = 2.69 \times 10^5 \times n^{3/2}AD^{1/2}v^{1/2}C$ (1), where I_p represents the peak current; n stands for the number of electrons transferred by $[\text{Fe}(\text{CN})_6]^{3-/4-}$ during the reaction ($n=1$); A represents the effective area of the electrode (cm^2); D represents the diffusion coefficient of potassium ferricyanide, which is $(7.6 \pm 0.02) \times 10^{-6} \text{ cm}^2/\text{s}$; v represents the sweep speed; C represents the concentration of the redox reactant ($5 \times 10^{-6} \text{ mol}/\text{cm}^3$). The order of effective area of different modified electrodes was as follows: AuNPs/GAs/GCE (0.182 cm^2) > GAs/GCE (0.142 cm^2) > Bare/GCE (0.115 cm^2). The above calculation results showed that the modification of the AuNPs/GAs composite further increased the effective area of the sensor electrode, and thus improved the electron transfer rate on the electrode surface, which intuitively showed an increase in conductivity.

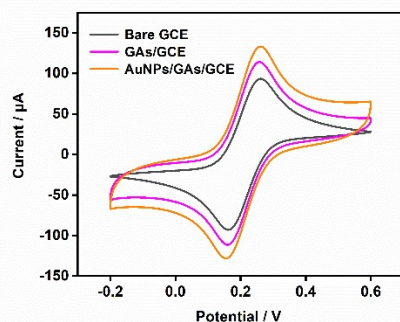


Fig. S2 CV curves of Bare GCE, GAs/GCE and AuNPs/GAs/GCE at 50 mV/s in 5

mM $[\text{Fe}(\text{CN})_6]^{3-/4-}$ containing 0.1 M KCl.

4.2 DPV responses of the Y-shaped structure on different sensing electrodes

To compare the signal differences of Y-shaped structures on different electrode surfaces, the control experiments with the Y-shaped structures in AuNPs/GCE and AuNPs/GAs/GCE were performed respectively. The results of the comparison were presented below. It was evident from **Fig. S3A** that there was a higher current response of the Y-shaped DNA structure on the surface of AuNPs/GAs-modified electrode compared to AuNPs alone due to the synergistic effect of AuNPs/GAs in improving electrode conductivity as well as increasing the amount of probe immobilized. Moreover, the signal gain generated on AuNPs/GAs/GCE (**Fig. S3B**, $\Delta I = 9.25 \mu\text{A}$) was more than four times that of AuNPs/GCE (**Fig. S3C**, $\Delta I = 2.16 \mu\text{A}$) with 50 nM target miR-21. The above data strongly proved that the introduction of GAs not only enhanced the conductivity of the electrode but also provided more attachment sites for AuNPs to immobilize more probe molecules, indicating that GAs plays an indispensable role in improving the sensitivity of the sensing electrode. Therefore, in our sensing strategy, the application of AuNPs/GAs as electrode material can indeed achieve the best detection effect for miR-21.

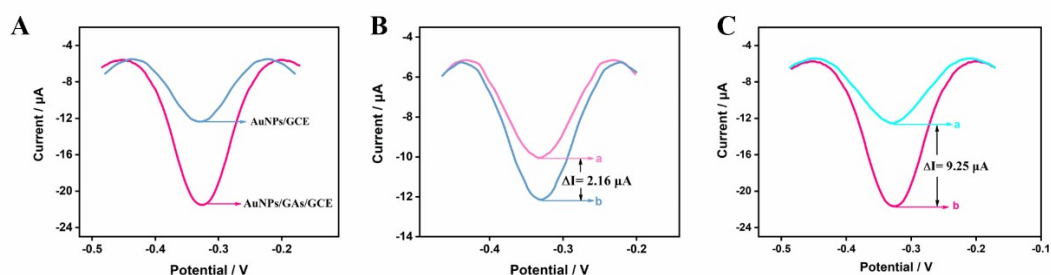


Fig.S3 Comparison of DPV responses of the Y-shaped structure in AuNPs/GCE and AuNPs/GAs/GCE (A); DPV responses differences of the as-prepared biosensor with zero analytes (curve a) and 50 nM target miR-21 (curve b) on different sensing electrode: AuNPs/GCE (B) and AuNPs/GAs/GCE (C).

4.3 Optimization of the experimental conditions

Prior to the quantification of miR-21 by applying the proposed sensing strategy, the amount of material dropped on the electrode and the incubation time of the probes (including the CHA and the Y-shaped DNA nanostructure) were optimized to achieve optimal analysis capability. Firstly, the amount of GAs loaded on the electrode had a great influence on the performance of the sensor. As shown in **Fig. S4A**, with the increase of GAs addition, the current value showed an upward trend until it exceeded 10 μL , and the current value tended to be gentle. Therefore, due to the limitation of the effective area of GCE, the best adding volume was 10 μL . Furthermore, the incubation time of the probes was optimized (**Fig. S4B** and **S4C**). **Fig. S4B** showed that the DPV response of the CHA reaction time reached a platform at 1.5 h from 0.5 h to 2.5 h, indicating that 1.5 h was the optimum reaction time. Analogously, the optimum

incubation time of the Y-shaped DNA nanostructure also was 1.5 h (**Fig. S4C**). Thus, the optimal DPV response was obtained when the material drop amount was 10 μL , the CHA hybridization time and the electrode capture incubating time of Y-shaped DNA nanostructure were 1.5 h respectively.

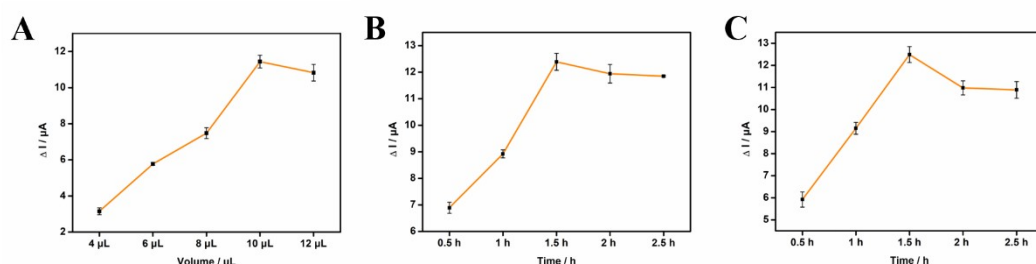


Fig. S4 Optimization of material addition (A) from 4 μL to 12 μL (including 4, 6, 8, 10 and 12 μL); Optimization of CHA reaction time (B) from 0.5 h to 2.5 h (including 0.5, 1, 1.5, 2 and 2.5 h) and Optimization of the hybridization time of Y-shaped DNA nanostructure (C) from 0.5 h to 2.5 h (including 0.5, 1, 1.5, 2 and 2.5 h).

Table S2. Comparison with other reported miR-21 detection methods.

Electrodes	Methods	Time for preparation	Time for detection	Linear range	LOD	References
TCEP/MB/GE	Electrochemistry	14 h	40 min	100 aM~100pM	77 aM	3
Au/GCE/TSDRs	Electrochemistry	14.5 h	2.5 h	1fM~10 nM	0.31 fM	4
M/MoS ₂ /Thi/Au NPs/GCE	Electrochemistry	4 h	1 h	100 fM~100 nM	26 fM	5
FeCN/GCE/Au NPs/Thi	Electrochemistry	13.5 h	4 h	1 fM~1 nM	0.853 fM	6
CdSNPs@CC/HCN/CHA	Photoelectrochemistry	15 h	2 h	1 fM~1 nM	0.41 fM	7
GE/DNAzyme Walker/MB	Electrochemistry	14.5 h	1 h	0~1 nM	0.27 fM	8
PTC-NH ₂ /luminol/CHA/TSDR	Electrochemiluminescence	15 h	3.5 h	100 aM~100 pM	33 aM	9
NFG/AgNPs/PANI	Electrochemistry	16.5 h	30 min	10 fM~10 aM	0.2 fM	10
GP/PPY/AuNPs/SPE/MB	Electrochemistry	5 h	1.5 h	1fM~1 nM	0.020 fM	11
AuNPs/GAs/GCE/CHA	Electrochemistry	4 h	2 h	5 fM~50 nM	14.7 aM	This work

4.4 Practical analysis of the designed biosensor in normal human serum

To evaluate the presence of the matrix effects in normal human serum, the calibration performed by applying the standard addition method (Fig. S5, curve a, calibration equation: $y = 1.151 \text{ Log } C + 20.33$, $R^2=0.9916$) and the calibration obtained for the standards (Fig. S5, curve b, calibration equation: $y = 1.209 \text{ Log } C + 21.16$, $R^2=0.9953$) were compared in Fig. S5. The matrix effects (ME) was evaluated by the slope values of the two calibration curves. The calculation process is as follows:

$$ME = \left(\frac{S_b}{S_a} - 1 \right) * 100\%$$

$$\rightarrow S_b=1.209, S_a=1.151$$

$$\rightarrow ME = \left(\frac{1.209}{1.151} - 1 \right) * 100\%$$

$$\rightarrow ME = (1.05039-1) * 100\% = 0.05039 * 100\% = 5.039\%$$

Therefore, the matrix effects in the standard addition method was 5.039%.

According to the calculation results, ME was between 0 and 20% ($0 < |ME| = 5.0395\% < 20\%$), indicating that the matrix effects existing in the standard addition method had low interference to the signal and can be neglected.

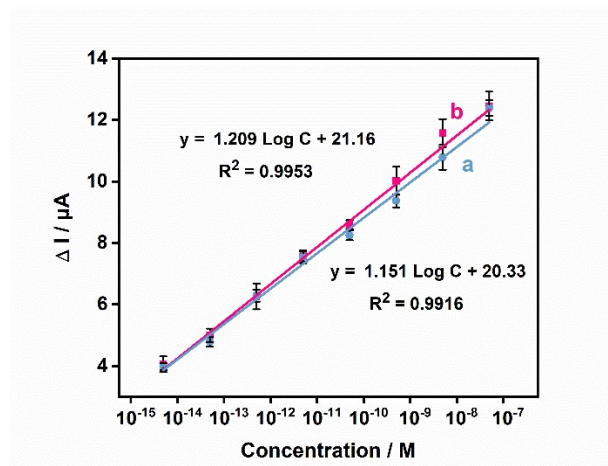


Fig. S5 Comparison of slope values of the calibration obtained for the standards (a) and of the calibration performed by applying the standard addition method (b).

In view of the high sensitivity and selectivity of the above sensor strategy, different concentrations of miR-21 (0.5 nM, 5 nM and 50 nM) were added into the 30-fold diluted normal human serum to calculate the recovery. **Table S3** clearly showed that recoveries of miR-21 at different concentrations ranged from 98.40 % to 107.4 % with RSD ranging from 0.6700 % to 3.770 %, suggesting the great practical application

potential in complex biological samples.

Table S3. Analysis result of the designed biosensor in normal human serum (n = 3).

Samples	Added (nM)	Measured (nM) (mean ± SD)	Recovery (%) (mean ± SD)	RSD (%)
1	0.5000	0.5370 ± 0.1650	107.4 ± 0.1650	1.710
2	5.000	5.350 ± 0.07210	107.0 ± 0.07210	0.6700
3	50.00	49.20 ± 0.4493	98.40 ± 0.4493	3.770

References

1. Z. Ning, E. Yang, Y. Zheng, M. Chen, G. Wu, Y. Zhang and Y. Shen, *Analytical Chemistry*, 2021, **93**, 8971-8977.
2. J. Dong, L. Wen, H. Yang, J. Zhao, C. He, Z. Hu, L. Peng, C. Hou and D. Huo, *Analytical Chemistry*, 2022, **94**, 5846-5855.
3. Z. Hu, B. Zhao, P. Miao, X. Hou and L. J. J. o. E. C. Feng, 2020, **880**, 114861.
4. Zhang, Xiaolong, Yang, Zhehan, Chang, Yuanyuan, Qing, Min, Yuan and R. J. A. Chemistry, 2018.
5. J. Zhao, C. He, W. Wu, H. Yang, J. Dong, L. Wen, Z. Hu, M. Yang, C. Hou and D. Huo, *Talanta*, 2022, **237**, 122927.
6. L. Cui, M. Wang, B. Sun, S. Ai, S. Wang and C. Y. Zhang, *Chem Commun (Camb)*, 2019, **55**, 1172-1175.
7. Y. Zhao, J. Xiang, H. Cheng, X. Liu and F. Li, *Biosens Bioelectron*, 2021, **194**, 113581.
8. Y. Xue, Y. Wang, S. Feng, M. Yan, J. Huang and X. Yang, *Anal Chem*, 2021, DOI: 10.1021/acs.analchem.1c01522.
9. W. Liu, A. Chen, S. Li, K. Peng, Y. Chai and R. Yuan, *Analytical Chemistry*, 2019, **91**, 1516-1523.
10. R. Salahandish, A. Ghaffarinejad, E. Omidinia, H. Zargartalebi, K. Majidzadeh-A, S. M. Naghib and A. Sanati-Nezhad, *Biosensors and Bioelectronics*, 2018, **120**, 129-136.
11. C. Pothipor, N. Aroonyadet, S. Bamrungsap, J. Jakmunee and K. Ounnunkad, *Analyst*, 2021, **146**, 2679-2688.